Low-Temperature Oxygen Migration and Negative Thermal Expansion in $ZrW_{2-x}Mo_xO_8$

J. S. O. Evans,*,† P. A. Hanson,† R. M. Ibberson,‡ N. Duan,§ U. Kameswari,§ and A. W. Sleight§

Contribution from the Department of Chemistry, University of Durham, Science Laboratories, South Road, Durham DH1 3LE, UK, ISIS Facility, Rutherford Appleton Laboratory, Chilton, Didcot, UK, and Department of Chemistry, Oregon State University, Corvallis, Oregon 97331

Received April 17, 2000

Abstract: The ZrW_2O_8 family of materials has been shown to display the unusual property of an isotropic bulk contraction in volume as a function of temperature. We report here on negative thermal expansion properties and oxygen migration at very low temperatures in $ZrW_{2-x}Mo_xO_8$ phases. $ZrWMoO_8$ shows significant negative thermal expansion ($\alpha_l = -8.7 \times 10^{-6}$ K^{-1}) and oxygen migration at temperatures as low as 200 K with an activation energy of 0.23 eV. We are unaware of oxygen migration at such low temperatures in other electronic insulators. The low-temperature migration is associated with an order−disorder transition between the α and β forms of the material with $\Delta V_{disorder} = -0.24\%$. A negative volume change for an order−disorder transition is unusual.

Introduction

The recent description of significant isotropic negative thermal expansion (NTE) in cubic ZrW_2O_8 over a wide temperature range has stimulated considerable interest in this topic.[1−3] NTE materials have a number of potential applications, the most obvious being in the production of composite bodies with precisely controllable positive, negative, or zero coefficients of thermal expansion. Such composites would find use in optical, electronic, and engineering applications. To date, most attention has been concentrated on the contraction properties of these materials. Here we report on the observation of NTE and oxygen mobility at unusually low temperatures in $ZrWMoO_8$; this mobility is related to an order−disorder phase transition in the material. Oxide ion mobility in ceramics has a number of potential areas of application including gas sensors, oxidation catalysis, and in fuel cells.

Many of the unusual properties of ZrW_2O_8 can be directly related to its crystal structure (Figure 1), which contains corner sharing ZrO_6 octahedra and WO_4 tetrahedra. The ZrO_6 octahedra share all six corners with WO_4 tetrahedra, whereas WO_4 tetrahedra share only three of their four corners with ZrO_6 octahedra. Six of the eight oxygens in each formula unit are thus in two-coordinate Zr−O−W bridges. The arrangement of the WO_4 groups is such that pairs of tetrahedra lie along the main 3-fold body diagonal of the cubic unit cell. One oxygen lies in an asymmetric W···O−W bridge with one very long (2.40 Å) and one short (1.72 Å) bond to the tetrahedral metal. The final oxygen atom, however, is strictly one coordinate and is bonded to a single W atom. The openness of this structure is perhaps one reason α-ZrW_2O_8 (ρ = 5.08 g cm^{-3}) is only metastable at temperatures below 1400 K with respect to the more condensed binaries ZrO_2 (ρ = 5.83 g cm^{-3}) and WO_3 (ρ = 7.19 g cm^{-3}). A second reason for instability is the unusually low coordination environment of one oxygen atom. In α-ZrW_2O_8 this low-coordinate oxygen is associated with the occurrence of an ambient pressure phase transition to a dynamically disordered state (β-ZrW_2O_8) at around 448 K and to a more dense phase (γ-ZrW_2O_8) at 300 K and around 0.3 GPa.[4]

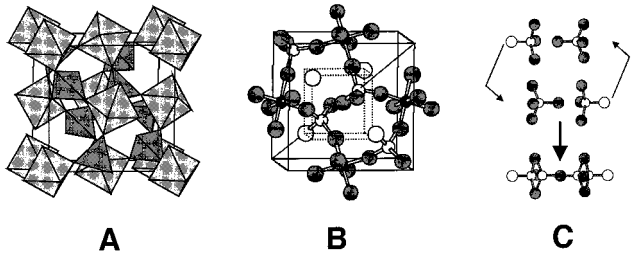

Figure 1. The structure of α-ZrM_2O_8. (A) A polyhedral representation showing ZrO_6 octahedra and MO_4 tetrahedra. (B) A ball-and-stick representation of a section of the structure; Zr is shown as small black spheres, M as small light spheres, one-coordinate oxygen atoms as larger open spheres, and two-coordinate oxygen as large gray spheres; $^1/_8$th of the face-centered lattice on which the one coordinate atoms lie is shown with dotted lines. (C) Schematic representation of pairs of MO_4 tetrahedra in the structure (for example those on the main body diagonal of the structure in part B), and their disorder in the high-temperature β form of the material.

The ambient pressure phase transition can be understood in a number of different ways. In low-temperature α-ZrW_2O_8 the one-coordinate oxygen atoms can be described as lying on a face-centered cubic lattice with its origin at ∼($^1/_4$, $^1/_4$, $^1/_4$) of the unit cell depicted in Figure 1. In the high-temperature β structure the oxygens are dynamically disordered over the full

* To whom correspondence should be addressed.
† University of Durham. Phone: 0191 374-3113. Fax: 0191 386 1127. E-mail: john.evans@durham.ac.uk.
‡ Rutherford Appleton Laboratory.
§ Oregon State University.

(1) Mary, T. A.; Evans, J. S. O.; Vogt, T.; Sleight, A. W. *Science* **1996**, *272*, 90−92.
(2) Evans, J. S. O.; Mary, T. A.; Vogt, T.; Subramanian, M. A.; Sleight, A. W. *Chem. Mater.* **1996**, *8*, 2809−2823.
(3) Evans, J. S. O. *J. Chem. Soc., Dalton Trans.* **1999**, 3317−3326.
(4) Evans, J. S. O.; Hu, Z.; Jorgensen, J. D.; Argyriou, D. N.; Short, S.; Sleight, A. W. *Science* **1997**, *275*, 61−65.

10.1021/ja0013428 CCC: $19.00
Published on Web 08/26/2000

and empty sites of this lattice. An alternative description is in terms of the pairs of 2(WO_4) tetrahedra shown in Figure 1C. In the low-temperature structure these tetrahedra all "point" in a definite direction. If one envisages a 4.6 Å hop of the terminal oxygen atom of one 2(WO_4) pair (e.g. that at ~($^3/_4$, $^3/_4$, $^1/_4$) of Figure 1B) to the empty end of a second pair (e.g. the vacant site at ~($^3/_4$, $^3/_4$, $^3/_4$)) followed by a 0.26 Å migration of the W···O−W bridging oxygen and migration of the original terminal oxygen atom of the second pair, one effectively reverses the direction in which the 2(WO_4) pair points. Borrowing the language of organic chemistry, this can be described as a series of coupled S_N2 reactions. In the high-temperature structure of β-ZrW_2O_8 this process occurs in a dynamic fashion.

Despite constraints imposed by the metastable nature of ZrM_2O_8 materials, it has recently been shown that it is possible to prepare $ZrW_{2-x}Mo_xO_8$ phases over the entire composition range $0 \leq x \leq 2$.[5−7] In this paper we report results of variable-temperature neutron diffraction experiments, which have been used to investigate details of the structures and thermal expansion properties of two important members of this series ($x = 1$, $ZrWMoO_8$; and $x = 2$, $ZrMo_2O_8$). These investigations have shown that both these materials show strong isotropic negative thermal expansion over a wide temperature range. In addition, we show that $ZrWMoO_8$ undergoes a phase transition from the disordered β form to the ordered α form at around 270 K. Temperature−time dependent diffraction studies have been used to follow the kinetics of the phase transition, and reveal the onset of oxygen migration at unusually low temperatures in this material.

Experimental Details

Cubic $ZrWMoO_8$ was prepared by literature methods.[6] Chemical analysis of the sample used for diffraction studies gave a W:Mo ratio of 1:1.1(5). Cubic $ZrMo_2O_8$ was prepared using a modification of the published synthesis.[8] $ZrMo_2O_7(OH)_2 \cdot 2H_2O$ was prepared according to the method of Clearfield[9] and decomposed at 723 K to produce a mixed-phase sample containing both cubic (78.2% by mass) and trigonal (21.8%) $ZrMo_2O_8$. In our hands the temperature required for formation of the cubic phase was significantly higher than that reported by Lind (633 K).[8]

Powder neutron diffraction data were recorded using the High-Resolution Powder Diffractometer (HRPD) at the ISIS pulsed source of the Rutherford Appleton Laboratory (RAL), UK, over a time-of-flight range of 34000−114000 μs (d = 2.364 to 0.7050 Å). For $ZrWMoO_8$, 13.26 g of powdered material were packed into a 5.9 cm^3 rectangular can, cooled from 300 to 2 K in 1 h and 23 min, and held at 1.65 K for 4 h 44 min in an AS Scientific Instruments cryostat. Diffraction data were then recorded in 2 K intervals as the sample was warmed from 2 to 640 K. A total count time corresponding to 3 μAh (~340 s) was used at each temperature. With a 2 min equilibration time at each temperature, an average heating rate of 2 K every 471 s resulted. Minor dips in beam intensity led to 9 of the 320 runs taking ca. 700 s. A more extended beam loss led to a 45 min anneal at 310 K. No significant discontinuities are evident in refined structural parameters at these points. Data were also recorded as the sample was cooled from 639 to 99 K in 2 K steps. Beam fluctuations on cooling led to 9 runs with an average run time of 1000 s, and an extended (6.5 h) anneal at 377 K. No discontinuity in refined parameters was observed at these points. The sample was then cooled from 99 to 2 K in 1 h and 6 min and a final low-temperature data set recorded.

To provide data between 99 and 2 K and to investigate the influence of cooling rate on oxygen migration, neutron diffraction data were also collected on cooling a sample of $ZrWMoO_8$ in 2 K steps from 300 to 270 K (16.5 K h^{-1}), 1 K steps to 200 K (8.25 K h^{-1}), in 44 steps to 40 K (27 K h^{-1}), and finally 2 K steps from 40 to 4 K (16.5 K h^{-1}). The sample was thus cooled through the phase transition ($T_C \sim 270$ K) at approximately half the rate of the initial cooling experiment. Data sets were again collected for 3 μAh, resulting in an average time of 7 min 16 s at each experimental temperature.

For $ZrMo_2O_8$, 9 g of finely powdered material were again mounted in a rectangular sample can, cooled to 4 K in 27 min, and held at 4 K for 1.5 h. Diffraction data were collected for 3 μAh (310 ± 8 s) every 2 K from 4 to 450 K on warming, with a 2 min equilibration time at each temperature. Beam losses led to an extended sample anneal of 497 min at 196 K. Significant changes in thermal expansion properties were seen at this point. The sample was then cooled to 300 K in 1 h 22 min, held at this temperature for 15 min, and cooled in 4 K steps to 200 K, 8 K steps from 200 to 24, and 4 K steps to 4 K. Data were collected for a total of 6.6 μAh (ca. 11 min) on cooling, with a 3 min equilibration time at each temperature.

X-ray diffraction data were recorded on a Siemens d5005 diffractometer using Cu Kα radiation and a diffracted beam monochromator. Data were collected from 10 to 140° 2θ with a step size of 0.02° and a collection time of 40 s per step.

Diffraction data at each experimental temperature were analyzed using the Rietveld method within the GSAS software suite.[10] Refinement of this large number of data sets (869 refinements in total) was automated using local FORTRAN routines. Selected variables were parametrized using protocols described elsewhere.[11] Further details of structural analysis will be published elsewhere.

High-temperature complex impedance measurements were made with a Solartron 1260 impedance analyzer over a frequency range of 30 MHz to 1 Hz on a 1.74 mm thick pellet which had been sintered at 1120 °C for 50 s. Pt contacts of approximately 2000 Å thickness were placed on both sides of the pellet by electron beam evaporation. The pellet was held for 20 min at each temperature prior to measurement.

Results and Discussions

Initial X-ray and neutron diffraction studies revealed that $ZrWMoO_8$ has the disordered β-structure at room temperature and that the W:Mo ratio was 1:1.05(3), in good agreement with chemical analysis.[7] Thermal expansion and structural properties as a function of temperature were determined by neutron powder diffraction. A sample of $ZrWMoO_8$ was cooled rapidly from room temperature to 2 K and its neutron powder diffraction pattern was recorded. Rietveld refinement of this quenched sample showed the structure at 2 K was essentially unchanged from that determined at room temperature. 320 powder diffraction data sets were then recorded in 2 K intervals as the material was warmed from 2 to 640 K. Data were collected for 5.7 min at each temperature, followed by 2 min for sample heating and equilibration at the new temperature. The sample was then equilibrated at 640 K for 1 h and diffraction data collected as it was cooled in 2 K steps to 99 K, then rapidly to 2 K. A full anisotropic structure refinement was performed at each temperature using the Rietveld method[10] and data analysis strategies described elsewhere.[11]

The cubic unit cell parameter of β-$ZrWMoO_8$ as a function of temperature is shown in Figure 2. On warming a smooth, continuous contraction is observed from the lowest temperatures measured. The linear coefficient of thermal expansion between

(5) Wilkinson, A. P.; Lind, C.; Pattanaik, S. *Chem. Mater.* **1999**, *11*, 101−108.
(6) Closmann, C.; Sleight, A. W.; Haygarth, J. C. *J. Solid State Chem.* **1998**, *139*, 424−426.
(7) Kameswari, U.; Sleight, A. W.; Evans, J. S. O. *Int. J. Inorg. Mater.* **2000**, accepted for publication.
(8) Lind, C.; Wilkinson, A. P.; Hu, Z. B.; Short, S.; Jorgensen, J. D. *Chem. Mater.* **1998**, *10*, 2335.
(9) Clearfield, A.; Blessing, R. H. *J. Inorg. Nucl. Chem.* **1972**, *34*, 2643−2663.
(10) Larson, A. C.; Dreele; R.B., V. Los Alamos Internal Report No. 86-748, 1994.
(11) Evans, J. S. O.; David, W. I. F.; Sleight, A. W. *Acta Crystallogr. B* **1999**, *55*, 333−340.

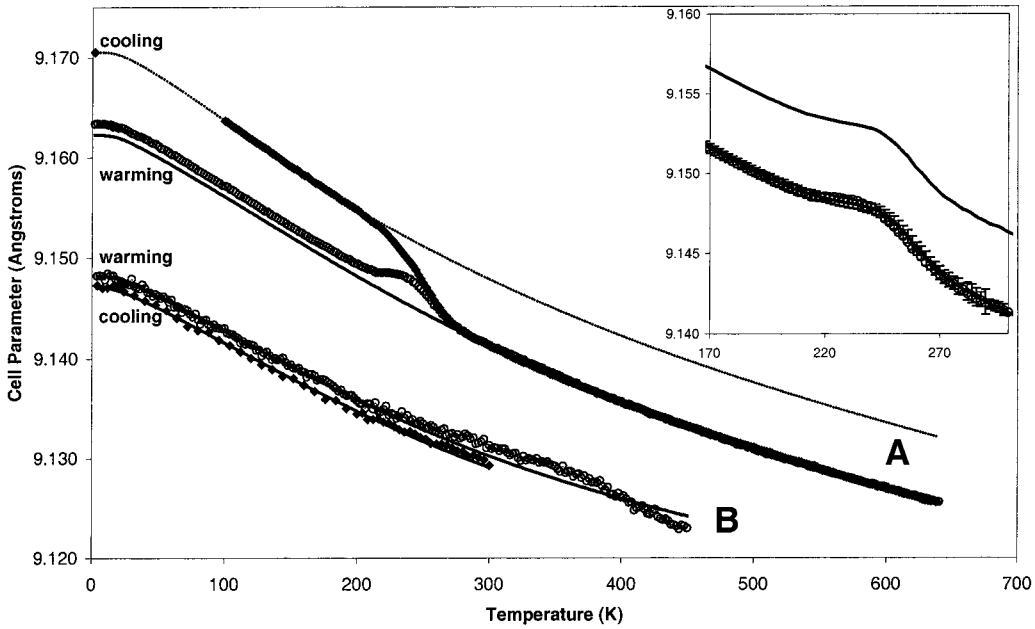

Figure 2. The cubic cell parameter of (A) $ZrWMoO_8$ on warming (open points) and cooling (closed points). A typical Rietveld uncertainty on an individual point is 4×10^{-5} Å, though the true precision is probably lower (see text). The solid line represents the thermal expansion of a hypothetical fully disordered sample of β-$ZrWMoO_8$, the dashed line a sample of ordered α-$ZrWMoO_8$. The inset shows the fitted cell parameter in the region of the phase transition; the solid line has been calculated using the parameters of Table 1 and an activation energy of 0.23 eV, and is also shown offset by 0.005 Å for clarity. Bars on the calculated line estimate uncertainty in the activated part of the model, which increases as T_C is approached. (B) Unit cell parameter data for $ZrMo_2O_8$ on warming (open points) and cooling (closed points). The solid lines represent a model with Einstein temperatures fixed at values comparable to those obtained for $ZrWMoO_8$ where higher quality data are available over a wider temperature range and are intended as a guide to the eye.

2 and 200 K is -7.69×10^{-6} K^{-1}.[12] This compares with $\alpha_l = -8.86 \times 10^{-6}$ K^{-1} for α-ZrW_2O_8 over the same temperature range. The shape of the cell parameter curve suggests a similar mechanism for thermal contraction as proposed for ZrW_2O_8. Inelastic neutron scattering,[13,14] heat capacity measurements,[15] analysis of thermal expansion curves,[16] and calculations[17,18] have all suggested that these materials have a family of vibrational modes with large negative Gruneisen parameters and energies in the region of 1.5 to 8.5 meV that dominate their overall thermal expansion properties. These modes can be thought of as librational and translational modes of essentially undistorted ZrO_6 and WO_4 polyhedra. On a local level, such modes involve transverse motions of Zr−O−M bridges. In the absence of significant expansion of individual metal-to-oxygen bond distances, such modes will naturally contract Zr−M distances and lead to NTE. Further discussion has been given elsewhere.[3]

From around 200 K, however, there is a marked deviation in the temperature dependence of the cell parameter (a_{warm}), and a "hump" is seen in its behavior. By 280 K the cell parameter has returned to its expected value. On cooling from 640 K the cell parameter, a_{cool}, initially matches a_{warm} extremely closely, with a_{cool} and a_{warm} values between 638 and 300 K lying within 2×10^{-4} Å of each other. This figure gives a more realistic estimate of the true precision of the cell parameter determination (which depends on the precision of the temperature control) than the Rietveld esd of 4×10^{-5} Å. At around 270 K, however, a marked divergence between a_{warm} and a_{cool} is observed. By 2 K the cell parameter of the slow-cooled sample is some 0.0070 Å larger than that of the quenched sample. The slow-cooled sample has a coefficient of thermal expansion of -8.69×10^{-6} K^{-1} between 200 and 2 K, more negative than that of a quenched sample over the same range.

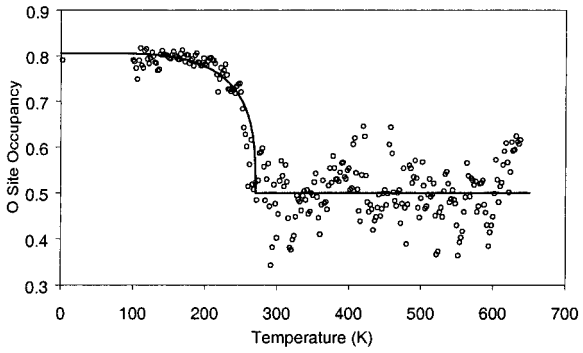

Figure 3. Fractional occupancy of the excess oxygen site on slow cooling $ZrWMoO_8$ obtained by Rietveld refinement in space group $P2_13$. The solid line represents a fit to a simple 3D cubic Ising model of the phase transition. Above T_C the true space group is $Pa\bar{3}$, and the occupancy is required by symmetry to be 0.5. This parameter is therefore ill-defined by the refinement strategy adopted, leading to the observed scatter.

This hysteresis in the cell parameter suggests that on slow cooling β-$ZrWMoO_8$ undergoes a phase transition to the ordered α-ZrM_2O_8 structure type. This phase transition (Figure 1C) involves the ordering of the one-coordinate oxygen atoms in the structure. Rietveld refinement of each individual data set allows this oxygen ordering to be followed. Figure 3 shows the fractional occupancy of the majority oxygen site as a function of temperature. The refined data follow a simple theoretical

(12) The coefficient of thermal expansion, α_l, is defined here as $\alpha_l = l_T - l_0/l_0(T - T_0)$, and will therefore depend on the temperature range used.

(13) Ernst, G.; Broholm, C.; Kowach, G. R.; Ramirez, A. P. *Nature* **1998**, *396*, 147−149.
(14) Wang, K.; Reeber, R. R. *Appl. Phys. Lett.* **2000**, *76*, 2203−2204.
(15) Ramirez, A. P.; Kowach, G. R. *Phys. Rev. Lett.* **1998**, *80*, 4903−4906.
(16) David, W. I. F.; Evans, J. S. O.; Sleight, A. W. *Europhys. Lett.* **1999**, *46*, 661−669.
(17) Mittal, R.; Chaplot, S. L. *Phys. Rev. B* **1999**, *60*, 7234−7237.
(18) Pryde, A. K. A.; Hammonds, K. D.; Dove, M. T.; Heine, V.; Gale, J. D.; Warren, M. C. *J. Phys. C* **1996**, *8*, 10973−10982.

model for such a transition well.[11] Oxygen ordering in slow-cooled $ZrWMoO_8$, in contrast to ZrW_2O_8, is not complete even at 2 K, the fractional occupancy of the favored site reaching only 0.80. There are several possible explanations for this lack of complete ordering. One possibility is that it reflects the inherent disorder of Mo and W on the tetrahedral sites of $ZrWMoO_8$. A given "pair" of tetrahedral sites may locally be W_2O_8, $WMoO_8$, or Mo_2O_8. These three possibilities, together with the far greater number of possibilities for 2nd nearest neighbor M_2O_8 groups, will lead to oxygen sites with a range of local potentials. This could perhaps lead to frustration of the oxygen ordering. A second possibility is that the introduction of Mo lowers the phase transition temperature to such an extent that the kinetics of O migration at 200 K are insufficient to allow further ordering. Slow cooling through the phase transition at half the rate of the initial experiment showed no increase in oxygen ordering (in fact a slightly lower degree of ordering was observed).[19] However, significantly slower cooling rates (not possible during neutron diffraction experiments) would be required to fully investigate this phenomenon. It is clear, however, that the introduction of 50% Mo on the tetrahedral sites of $ZrWMoO_8$ has lowered the phase transition temperature sufficiently that we can successfully stabilize both α and β forms of the material at the same temperature. The cell parameter difference of the two forms corresponds to a $\Delta V_{disorder}$ ($\Delta V_{disorder} = V_{disordered} - V_{ordered}$) of -0.24% at 0 K. This figure is an underestimate of the value for a fully ordered to fully disordered transition.

The "hump" observed in the cell parameter on warming the quenched sample can be understood in terms of the oxygen-ordering phase transition. As the material is warmed toward 200 K there is sufficient thermal energy for the quenched disordered oxygen array to order toward the more thermodynamically stable α form. However, the nature of the experiment (in which the sample is held at a given temperature, T, for only 471 s) means that insufficient time is allowed for the sample to reach its equilibrium structure (and hence cell parameter) at temperatures below ~270 K. For this reason, the variation of the cell parameter during a single experimental temperature interval contains information concerning the rate of the oxygen ordering process at that temperature.

The temperature dependence of the unit cell parameter data has been parametrized using expressions derived from the Gruneisen approximation, which relates the thermal expansion to the heat capacity at constant volume, $C_V(T)$, the isothermal compressibility, K_0, and the volume, V_0, at absolute zero: $\alpha(T) = \gamma K_0 C_V(T)/V_0$.[20] For the purposes of this analysis, the heat capacity, $C_V(T)$, has been approximated by two Einstein contributions, one weighted with a negative Gruneisen parameter to model low-energy phonons that tend to contract the lattice, and one with a positive contribution to model those modes that tend to expand the lattice. Despite the gross approximation to the true phonon density of states, such a model is able to parametrize the observed cell parameter extremely well (Figure 2), with a low number of refined parameters.

To obtain a good fit to the cell parameter on warming (excluding the "humped" region between 200 and 300 K) it was necessary to introduce a constant offset in the cell parameter data below 200 K. This suggests that even during the rapid initial cooling of the sample (220 K h^{-1}) some oxygen ordering occurred. The overall warming cell parameter was thus described by an expression $a_{warm}(T) = a_0 + E_1 + E_2 + \delta a_{warm}$, where a_0 is the cell parameter at 0 K, E_1 and E_2 represent the two Einstein contributions to the thermal expansion, and δa_{warm} ($\delta a_{warm} = 0$ for $T > T_C$) represents the increase in cell parameter due to partial ordering during quench cooling. The same function was used to model the cooling cell parameter, $a_{cool}(T)$ above T_C. Below T_C α-$ZrWMoO_8$ has a significantly more negative thermal expansion coefficient, presumably due to the more open nature of the structure, and was fitted to an expression $a_{cool}(T) = a_0 + E_3 + E_4 + \delta a_{cool}$. From this parametrization (Table 1) one can derive approximate expressions for the cell parameter of a (hypothetical) fully disordered sample of β-$ZrWMoO_8$ over the entire temperature range.

Table 1. Coefficients in the Expression $\ln(\alpha_{phonon}/\alpha_0) = c_1\theta_1/[\exp(\theta_1/T) - 1] + c_2\theta_2/[\exp(\theta_2/T) - 1]$, where $\alpha(T) = \alpha_{phonon} + \delta\alpha$, Used To Parametrize the Phonon Contributions to the Overall Cell Parameter, $a(T)$[a]

	quenched sample (warming)	slow cooled sample (cooling)
$a_0(\beta$-$ZrWMoO_8)$ (Å)	9.16226	
δa (Å)	0.00107	0.00826
$a(T=0\ K) = a_0 + \delta a$ (Å)	9.16333	9.17052
θ_1 (K)	55.3	64.0
c_1 ($\times 10^{-7}$ K^{-1})	−90.3	−105
θ_2 (K)	1143.8	929.8
c_2 ($\times 10^{-7}$ K^{-1})	65.6	55.9

[a] Constants c_1 and c_2 are treated here as refineable parameters and approximate effects of the true phonon density of states, Gruneisen parameters, volume, and compressibility.

Since the cell parameter is measured far more precisely in a powder diffraction experiment than an oxygen site occupancy parameter can be refined, we have used the excess cell of the warmed sample over a hypothetical fully disordered material to give information about the oxygen ordering. If one assumes that the oxygen ordering depends on the (excess cell)$^{1/2}$, it can be shown that the extent of ordering, $f(T)$, at any temperature is given by

$$f(T) = \frac{\delta a_{warm}^{1/2}}{\delta a_{eqm}^{1/2}}$$

where δa_{warm} represents the excess cell parameter at a given temperature of the quenched sample over a fully disordered material on warming, and δa_{eqm} represents the excess cell parameter of a sample at equilibrium (assumed here to be the sample obtained on slow cooling). In a temperature−time experiment such as that performed here, the extent of ordering at any point will depend on the overall changes that have occurred at each preceding temperature, for the entire time of the experiment to date. If one assumes a simple first-order rate law, the rate expression for such a process can be shown to be given by

$$\exp(-k_T t) = 1 - \frac{\delta f(T)}{1 - \sum_{T=0}^{T-1} \delta f(T)}$$

where k_T is the first-order rate constant at a given temperature, $\delta f(T)$ represents the change in extent of ordering at temperature T, and $\sum_{T=0}^{T-1}\delta f(T)$ is the sum of changes in $f(T)$ at all preceding temperatures.[21] Under the assumption that $f(T)$ values can be extracted from the excess cell parameter, the "hump" of a_{warm}

(19) Cooling from 270 to 200 K at the slower rate of 8.25 K h^{-1} led to a majority site occupancy of 0.75. We believe that the degree of oxygen ordering may depend critically on the full thermal history of the sample.

(20) Reeber, R. R. *Phys. Status Solidi A* **1975**, *32*, 321.

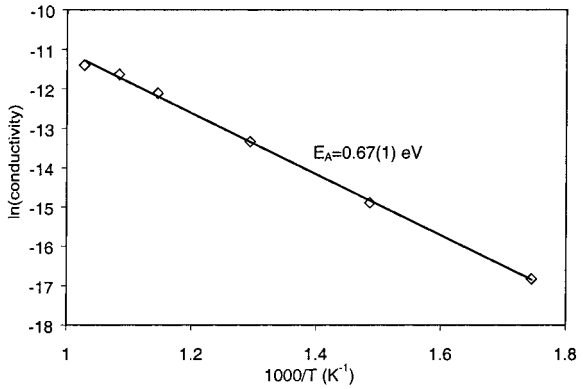

Figure 4. Arrhenius plot of ln(conductivity) against inverse temperature derived from high-temperature complex impedance measurements.

contains information about the rate constant at each experimental temperature. If one assumes a simple Arrhenius type behavior [$k_T = A \exp(-E_A/RT)$] then information about the activation energy of the process can be obtained. In fact the rate expressions can be fitted directly to the observed cell parameter, giving the fit of Figure 2 and values of $A = 11$ s^{-1} and $E_A = 0.23$ eV (22 kJ mol^{-1}). We estimate the error on E_A to be ± 0.05 eV.

The observation of bulk oxygen migration at such low temperatures in the solid state is unusual. Migration of excess oxygen has been reported at low temperature in certain nonstoichiometric systems related to the high-temperature cuprate superconductors. For example, compelling evidence for oxygen diffusion in $La_2CuO_{4+\delta}$ at low temperatures has been derived by magnetic susceptibility, neutron diffraction, and NQR measurements. Activation energies have been estimated at 0.24,[22] 0.25,[23] and 0.31 eV[24] by various techniques. The temperature at which significant mobility occurs has been quoted as occurring between 150 and 230 K, and is extremely technique dependent. Oxygen mobility has also been inferred from powder neutron diffraction measurements on $La_2NiO_{4+\delta}$ where phase transitions involving oxygen migration have been described at temperatures as low as 220 K.[25] Further support for the proposed oxygen migration model in $ZrWMoO_8$ comes from complex impedance measurements which show a conductivity of $\sigma \sim 10^{-6}$ Ω^{-1} cm^{-1} at around 700 K. A plot of ln σ against $1/T$ (Figure 4) suggests an activation energy of around 0.67 ± 0.1 eV at high temperature. Activation energies for oxygen migration are frequently temperature dependent, and depend on the specific phase in question. Given that the low-temperature experiment measures short-range oxygen migration to a thermodynamically more stable ordered material, whereas the high-temperature experiments presumably monitor a longer-range effect, these two values do not seem inconsistent.

Figure 2 also contains cell parameter data for $ZrMo_2O_8$, which have been recorded at considerably more temperatures than previously reported.[8] The material was again quench-cooled before warming gradually to 450 K, then cooling slowly from 300 K. Diffraction data suggest that the material retains the disordered β structure throughout. There are, however, clear discrepancies between warming and cooling cell parameters. In addition, a marked discontinuity was caused in the warming cell parameter by a 500 min anneal at 196 K. These observations provide further evidence that introduction of Mo on the tetrahedral site of these materials lowers the transition temperature to the ordered α-AM_2O_8 structure. The ordering temperature in $ZrMo_2O_8$ is presumably lower still than that of ZrW_2O_8 (448 K) or $ZrWMoO_8$ (270 K), and oxygen ordering is yet to be observed by ourselves or others.[8] The discontinuities and dependence on thermal history of the cell parameter of $ZrMo_2O_8$ do, however, provide indirect evidence that oxygen-ordering effects may also be important in this material.

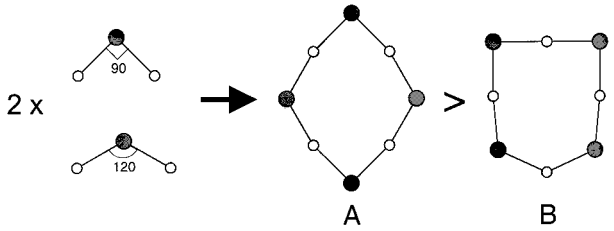

Figure 5. Schematic representation of how the area of a two-dimensional metal oxide ring depends on the sequence of bond angles around that ring. (A) A bond angle sequence of 90°, 120°, 90°, 120° gives a ring area of 4.3155 Å^2 (for a M−O distance of 1 Å), 0.8% larger than (B) a bond angle sequence of 90°, 90°, 120°, 120° (area = 4.2802 Å^2). Metal atoms are represented by small light circles and oxygen atoms large dark circles. Modeled after Hazen et al.[26]

The effect of both static and dynamic oxygen disorder in the ZrM_2O_8 materials is to cause a significant reduction in volume; the cell parameter at 0 K being some 0.0082 Å larger for an 80% ordered sample of $ZrWMoO_8$ than a disordered sample; $\Delta V_{\text{disorder}} = -0.24\%$. The observation of a decrease in cell volume at a temperature driven phase transition is somewhat unusual.[26] This phenomenon can, however, be rationalized by similar arguments used to understand the negative expansion coefficient. If one uses the thermodynamic relationship

$$\alpha_V = \frac{1}{V}\left(\frac{\partial V}{\partial T}\right)_P = K\left(\frac{\partial P}{\partial T}\right)_V = K\left(\frac{\partial S}{\partial V}\right)_T$$

we see that for materials with α_V negative S and V are anti-correlated.[27] One measure of disorder which may influence the volume of these framework materials is the regularity of the Zr−O−M bond angles. In the ordered ZrM_2O_8 structure there are two distinct Zr−O−M bond angles of ca. 154 and 173°. In the high-temperature dynamically disordered material, bond angles lose their individual identities and fluctuate between these extremes. In the statically disordered material, local disorder of oxygen sites will lead to a similar static disorder of Zr−O−M angles, a local entropic gain, and cause contraction of the material. The inference that the arrangement of Zr−O−M angles (determined in turn by O ordering) can influence the volume of these materials can perhaps be appreciated by the simple two-dimensional analogy of an 8-membered ring comprising 4 metal atoms and 4 two-coordinate bridging oxygen atoms (Figure 5). If this ring has two M−O−M bond angles of 90° and two of 120°, then the total area enclosed by the ring differs depending on the sequence of bond angles (a 90°, 120°, 90°, 120° sequence of bond angles around the ring having a ~1% smaller volume than 90°, 90°, 120°, 120°).[26] The cell volume of a framework material will therefore depend not only

(21) David, W. I. F.; Ibberson, R. M.; Matsuo, T. *Proc. R. Soc. London A* **1993**, *442*, 129−146.
(22) Chou, F. C.; Johnston, D. C. *Physical Review B−Condensed Matter* **1996**, *54*, 572−583.
(23) Reyes, A. P.; Hammel, P. C.; Ahrens, E. T.; Thompson, J. D.; Canfield, P. C.; Fisk, Z.; Schirber, J. E. *Journal of Physics and Chemistry of Solids* **1993**, *54*, 1393−1402.
(24) Kappesser, B.; Wipf, H.; Kremer, R. K. *Journal of Low-Temperature Physics* **1996**, *105*, 1481−1486.
(25) Tranquada, J. M.; Kong, Y.; Lorenzo, J. E.; Buttrey, D. J.; Rice, D. E.; Sachan, V. *Phys. Rev. B−Condensed Matter* **1994**, *50*, 6340−6351.
(26) Hazen, R. M.; Navrotsky, A. *Am. Mineral.* **1996**, *81*, 1021−1035.
(27) Landau, L. D.; Lifshits, E. M. *Statistical Physics*; Pergamon Press:, 1958.

Table 2. Linear Expansion Coefficients, α_l, and Cell Parameter at 0 K for $ZrW_{2-x}Mo_xO_8$ Samples[a]

material	*a* (0 K)	α_l ($\times 10^{-6}$ K^{-1})
ZrW_2O_8[11]	9.18000	−9.7
$ZrWMoO_8$ quenched	9.16333	−8.6
$ZrWMoO_8$ slow cool	9.16793	−9.4
$ZrMo_2O_8$ quenched	9.14820	−7.6
$ZrMo_2O_8$ slow cool	9.14721	−7.8

[a] Details of sample thermal histories are given in the text; values of α are quoted from 30 to 120 K for comparison.

on the value of the framework bond angles, but also on their arrangement in the structure. Similar arguments have been proposed to explain a negative $\Delta V_{disorder}$ in $RbAlSi_3O_8$.[26]

The structure adopted by ZrM_2O_8 at any temperature is clearly determined by several factors. From this experiment the ordered α-ZrM_2O_8 structure can be seen to be thermodynamically favored over β-ZrM_2O_8 at low temperatures, though it probably represents only one kinetically accessible local minimum on the free energy hypersurface. This stability is, at least in part, driven by the electrostatic ordering of the one-coordinate oxygen ions. Bond valence arguments [28,29] have shown, however, that oxygen is significantly underbonded at this site.[30] This presumably drives both the high-temperature and high-pressure phase transitions in these phases. There is clearly also an entropic contribution to the stability of the β-ZrM_2O_8 structure.

Table 2 contains linear expansion coefficient values for ZrW_2O_8,[11] the ordered and disordered forms of $ZrWMoO_8$, and the sample of $ZrMo_2O_8$ with two different thermal histories. The thermal expansion coefficient can be seen to correlate with the volume of the unit cell at low temperature. The larger the 0 K volume of the framework structure, the more negative the volume expansion coefficient. This presumably reflects the increased dominance of transverse modes with negative Gruneisen parameters to the overall thermal expansion in the more open materials.

Conclusion

This work has confirmed that the three members of the $ZrW_{2-x}Mo_xO_8$ series studied in detail to date exhibit strong, isotropic negative thermal expansion over a broad temperature range. The existence of oxygen ordering in $ZrWMoO_8$ has been shown for the first time, and we have demonstrated that oxygen migration can occur in this phase at temperatures as low as 200 K. The introduction of Mo lowers the transition temperature from the ordered to disordered structure significantly (448 to 270 K). The degree of oxygen ordering in these materials influences their unit cell volume, such that both phonon contributions and oxygen distribution must be considered when trying to understand their thermal contraction behavior.

Acknowledgment. We wish to acknowledge the EPSRC for access to neutron facilities, Mark Newmann of the Sante Fe Institute for providing the theoretical curve used in Figure 3, and a referee for helpful suggestions.

Supporting Information Available: Tables of unit cell parameters of both $ZrWMoO_8$ and $ZrMo_2O_8$ on warming and cooling (PDF). This material is available free of charge via the Internet at http://pubs.acs.org.

JA0013428

(28) Brese, N. E.; O'Keeffe, M. *Acta Crystallogr. B* **1991**, *47*, 192−197.

(29) Brown, I. D.; Altermatt, D. *Acta Crystallogr. B* **1985**, *41*, 244−247.

(30) Bond valences in α-ZrW_2O_8 have been shown to be 2.079, 2.072 (Zr−O−W), and 2.001 (W···O−W) for two-coordinate oxygens but only 1.784 for the one-coordinate oxygen.